Observations of the semidiurnal internal tide on the southern California slope and shelf

J. A. Lerczak
Department of Physical Oceanography, Woods Hole Oceanographic Institution, Woods Hole, Massachusetts, USA

C. D. Winant and M. C. Hendershott
Scripps Institution of Oceanography, University of California, San Diego, La Jolla, California, USA

Received 27 August 2001; revised 11 November 2002; accepted 18 November 2002; published 12 March 2003.

[1] We give a detailed description of the semidiurnal-band current and temperature variability observed during the Internal Waves on the Continental Margin (IWAVES) field experiments of 1996 and 1997 off of Mission Beach, California. This variability was dominated by the internal tide, and the structure of the internal tide on the slope and shelfbreak region was different from that on the narrow shelf. On the slope and shelfbreak, the internal tide was dominated by alongshore propagating coastal-trapped waves. In this region, semidiurnal-band currents were predominantly oriented in the alongshore direction. In the lower half of the water column at a water depth H of 350 m, current and temperature variability were consonant with a short wavelength ($\sim$8 km) bottom trapped wave propagating in the alongshore direction to the north. In the upper 120 m of the water column (above the depth of the shelfbreak), slope and shelfbreak currents were highly coherent with a zero phase lag; that is, there was no phase propagation in the cross-shore direction. On the narrow ($\sim$10 km) shelf, cross-shore currents u were much more energetic than on the slope and had the structure of a mode-one internal wave. The alongshore currents v decreased monotonically from the surface to the bottom of the water column with a phase that did not change with depth. The near-bottom u signal propagated toward the coast during all mooring deployments, faster in the summer than in the fall. The near-bottom u and mid-column temperature relative phase was neither consistent with a purely progressive nor a purely standing mode-one internal wave. We conclude that the internal tide on the shelf was partially reflected. *INDEX TERMS:* 4219 Oceanography: General: Continental shelf processes; 4544 Oceanography: Physical: Internal and inertial waves; 4560 Oceanography: Physical: Surface waves and tides (1255); 1255 Geodesy and Gravity: Tides—ocean (4560); *KEYWORDS:* internal tide, internal waves, continental shelf and slope circulation, coastal-trapped wave

Citation: Lerczak, J. A., C. D. Winant, and M. C. Hendershott, Observations of the semidiurnal internal tide on the southern California slope and shelf, *J. Geophys. Res.*, *108*(C3), 3068, doi:10.1029/2001JC001128, 2003.

1. Introduction

[2] We describe here the spatial and temporal structure of the semidiurnal-band current and isopycnal displacement variability observed on the narrow continental shelf and adjacent slope off of Mission Beach, California (Figure 1) during the Internal Waves on the Continental Margin (IWAVES) experiments of 1996 and 1997. Tidal-band variability usually exhibits complicated spatial and temporal behavior on and near continental shelves [*Wunsch*, 1975; *Hayes and Halpern*, 1976; *Torgrimson and Hickey*, 1979; *Winant and Bratkovich*, 1981; *Huthnance and Baines*, 1982; *Denbo and Allen*, 1984; *Bratkovich*, 1985; *Baines*, 1986; *Sherwin*, 1988; *Rosenfeld*, 1990; *Holloway*, 1994; *Holloway et al.*, 2001]. This is often due to the presence of an energetic internal tide.

0148-0227/03/2001JC001128$09.00

[3] Coastal internal tides are often described as cross-shore propagating mode-one internal waves [*Sherwin*, 1988; *Rosenfeld*, 1990; *Holloway*, 1994; *Holloway et al.*, 2001]. For this type of wave, there is no alongshore spatial dependence, and the inviscid, linear alongshore momentum equation is

$$v_t + fu = 0, \tag{1}$$

where u and v are the cross-shore and alongshore currents, respectively, and f is the inertial frequency. At all locations, u and v are 90° out of phase, clockwise polarized (in the Northern Hemisphere) and are related in amplitude by

$$\frac{|v|}{|u|} = \frac{f}{\sigma}, \tag{2}$$

where σ is the semidiurnal frequency ($f/\sigma = 0.56$ at the IWAVES study site). For this type of wave, currents (both u

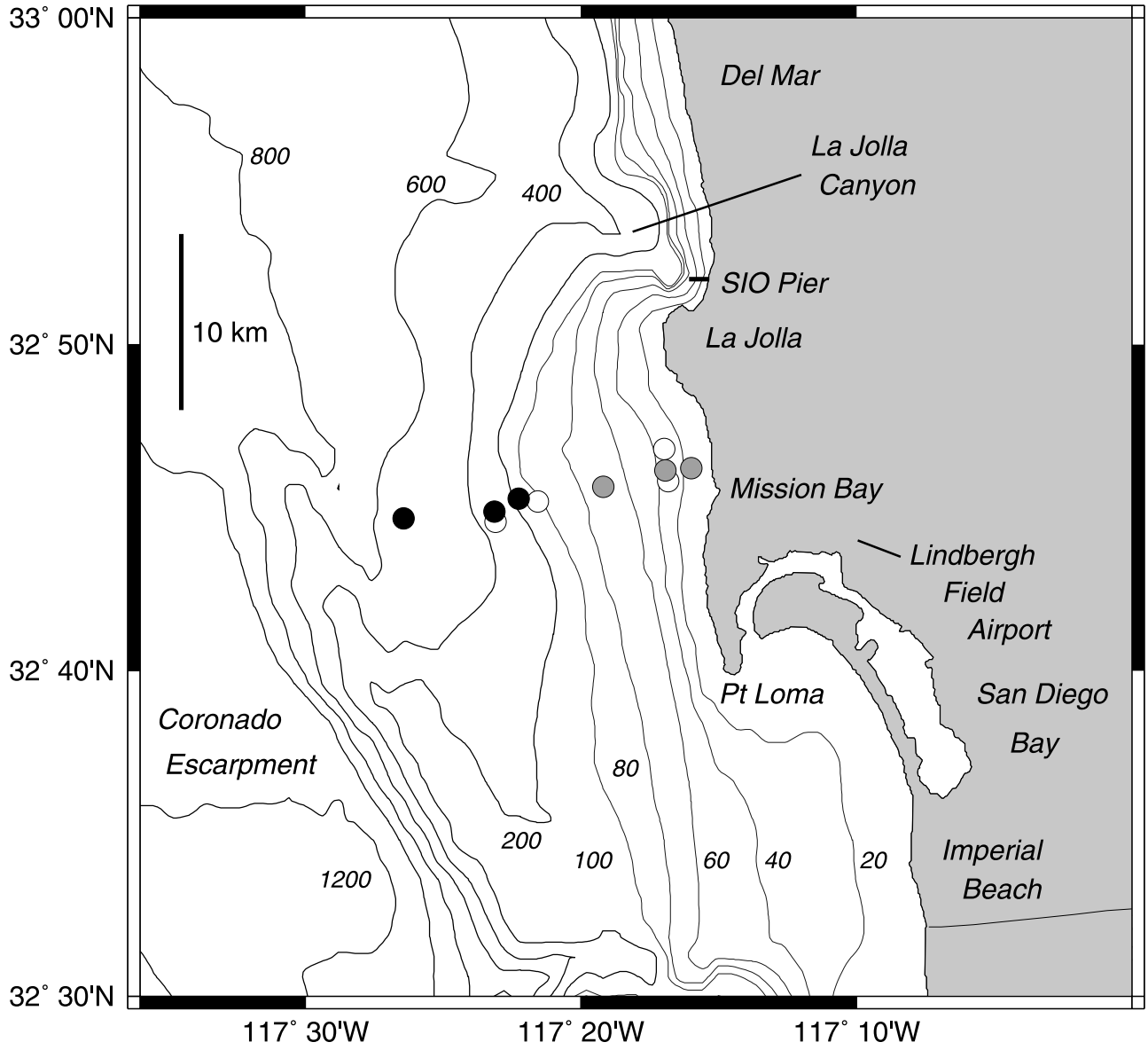

Figure 1. Internal Waves on the Continental Margin (IWAVES) study site. Circles mark the locations of the moorings of the summer arrays. Open circles mark moorings deployed in the summer of 1996; solid circles mark summer 1997 moorings; shaded circles mark moorings deployed in the summer of both years. Depths are given in meters. The 1996 and 1997 fall mooring deployments are not shown (see *Lerczak* [2000] for details).

and v) near the surface are 180° out of phase with respect to currents near the bottom of the water column.

[4] In contrast, an internal Kelvin wave trapped to the coast has motions that are linearly polarized in the alongshore direction ($u = 0$), and propagate along the coast with the coastline to the right (in the Northern Hemisphere; northward at the IWAVES study site). For a mode-one Kelvin wave, surface and bottom alongshore currents (v) are 180° out of phase. With realistic slope/shelf topography, coastal-trapped waves (CTWs) have a more complicated structure [*Huthnance*, 1978; *Ou*, 1980; *Ou and Beardsley*, 1980; *Dale and Sherwin*, 1996; *Dale et al.*, 2001]. Cross-shore currents may be nonzero. However, alongshore currents still tend to dominate the variability when the internal deformation radius is larger than the cross-shore scale of the continental slope [*Huthnance and Baines*, 1982]. Lines of constant phase can be complicated. Indeed, for realistic slope/shelf cross-sections, there can be locations on the shelf where there are no 180° vertical phase shifts in the currents and the motions, therefore, have a nonzero vertical mean [*Huthnance*, 1978; *Ou*, 1980; *Ou and Beardsley*, 1980; *Dale and Sherwin*, 1996; *Dale et al.*, 2001]. This can make the separation of the internal tide and the surface tide difficult, if not impossible. (By surface tide, we mean the astronomically-forced tidal motions that would exist in a homogeneous (unstratified) ocean and which force the internal tide in a stratified ocean.) While CTWs are not perfectly trapped at superinertial frequencies, nearly-trapped waves can exist and propagate along the coast for long distances before losing their energy by scattering into freely

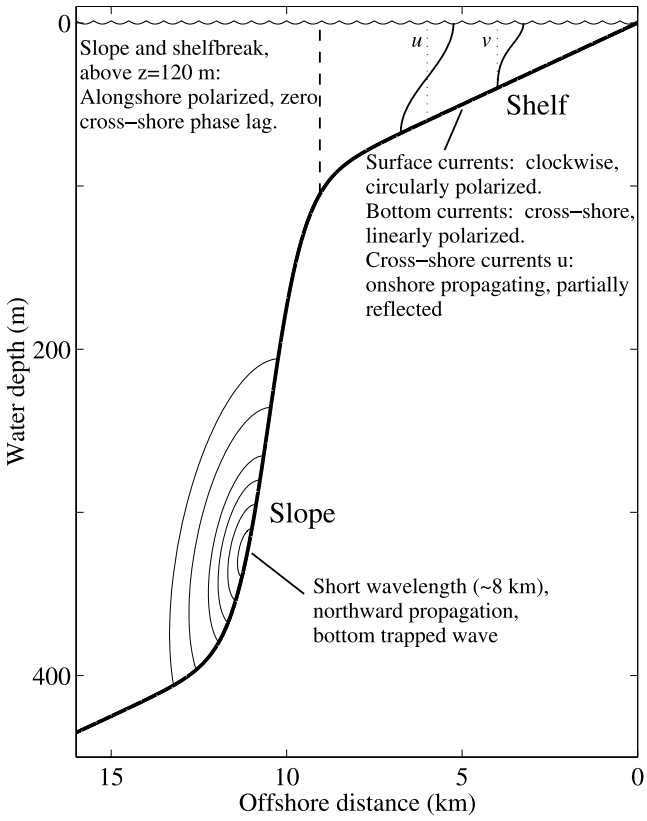

Figure 2. Summary of the structure of the internal tide observed during the IWAVES field studies and reported on in this paper.

propagating internal waves [*Chapman*, 1982a, 1982b; *Dale and Sherwin*, 1996; *Dale et al.*, 2001].

[5] For the reasons noted above, we do not decompose the currents observed during IWAVES into a vertical average and residual currents as others have in order to separate the surface from the internal tide [*Rosenfeld*, 1990; *Holloway et al.*, 2001; *Colosi et al.*, 2001]. From the vertical structure of the currents, it is apparent that the semidiurnal variability was dominated by the internal tide.

[6] We contrast the coastal internal wave models (mode-one internal waves and CTWs) with the observations made during IWAVES. To help guide the reader through the analyses in the following sections, we begin with a preview of the salient results (Figure 2).

[7] The nature of the internal tide on the slope and shelfbreak was very different from that on the shelf, and we describe the structure at these two locations separately. On the slope and shelfbreak (water depth H between 500 and 120 m), semidiurnal-band alongshore currents v were generally much more energetic than cross-shore currents u. This was particularly true near the surface and at depths greater than 200 m, where the currents were polarized in the alongshore direction. Alongshore currents were strongest at H = 120 and 350 m and were weaker further offshore (H = 500 m). At depths z less than 120 m, currents on the slope and shelfbreak (H = 350 and 120 m) were highly coherent and had a zero phase lag in the cross-shore direction. This behavior (alongshore polarization, zero cross-shore phase lag, and decay away from the shelfbreak) is consonant with a coastal-trapped wave. For z > 200 m at the 350 m mooring, variance in v was large near the bottom and decayed exponentially toward the surface. As at the surface, current ellipses here were polarized in the alongshore direction. The semidiurnal-band relative phase between v and temperature was consistent with northward phase propagation and the overall structure was consistent with a short alongshore wavelength (∼8 km) bottom trapped wave (BTW) [*Rhines*, 1970]. Semidiurnal currents here were much better correlated with the surface tide than those anywhere else in the array, so much so that deep semidiurnal currents (unlike at all other regions sampled) exhibited a spring/neap cycle analogous to that of the surface tide.

[8] On the shelf, semidiurnal-band variance in u was greatest at the top and bottom of the water column and minimal at mid-depth, and there was a sharp 180° phase shift between the top and the bottom of the water column. Near the surface, u and v were 90° out of phase and were clockwise polarized. This much is broadly consonant with a mode-one internal wave over the shelf. However, the vertical structure of variance in v was not at all what the mode-one picture would predict. Instead, that variance generally decreased from the surface to the bottom, and there was very little phase variation from top to bottom. For u, there was a clear sense of shoreward phase progression at speeds comparable to that of a freely propagating mode-one internal wave, but there was a seasonal dependence to the phase speed (faster in the summer than in the fall). The relative phase between bottom u and mid-column temperature fluctuations, T, was neither consistent with a purely progressive nor a purely standing mode-one internal wave and suggests that the internal tide was partially reflected on the shelf. Seasonal changes in the cross-shore phase speed and the u/T phase relationship were consistent with the reflection coefficient being higher in the summer than in the fall.

2. Observations

[9] The IWAVES study site (Figure 1) was 25 km to the south of the 1977–1979 field studies off Del Mar, California reported by *Winant and Bratkovich* [1981] and *Bratkovich* [1985]. (Details of the IWAVES field experiments are given by *Lerczak* [2000].) The inshore limit of the IWAVES arrays (at a water depth, H, of 15 m) was at the same location as that of the internal wave experiments reported by *La Fond* [1962], *Cairns* [1967], and *Winant and Olson* [1976]. Our studies took place during the summer and fall months of 1996 and 1997. Arrays were deployed twice each year with different configurations. From approximately the end of June to the beginning of September each year, the array spanned water depths from 15 m to 500 m, covering a cross-shore range of ∼16 km. From late summer to mid-fall, moorings were tightly spaced in shallow, nearshore depths ranging from 15 to 30 m (except for a mooring at H = 100 m deployed during the fall of 1996).

[10] Each mooring was instrumented with at least one acoustic Doppler current profiler (ADCP) to measure velocities as a function of depth. On the shelf, which we define as the shoreward shoaling region with H < 120 m

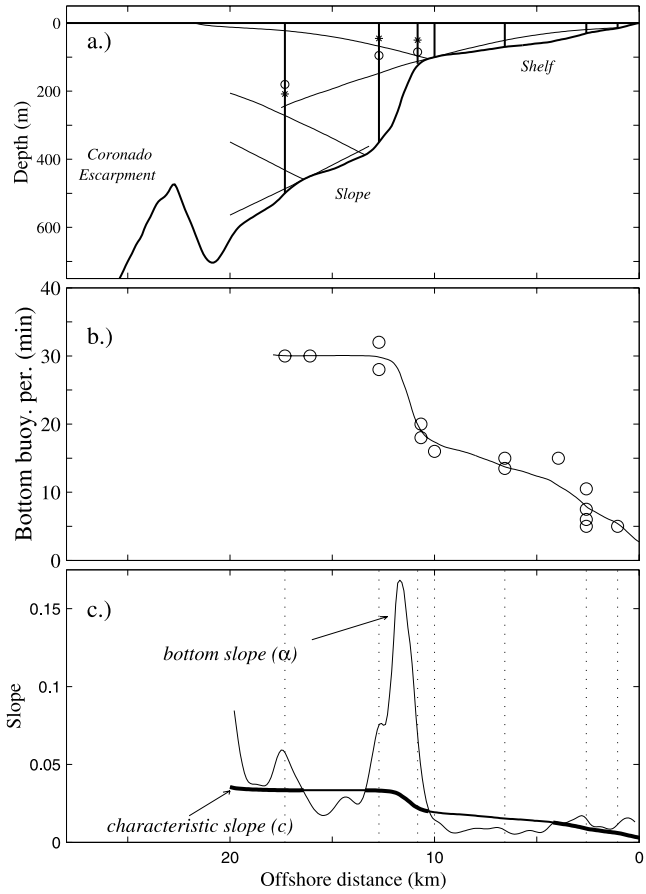

Figure 3. (a) Bathymetry along the cross-shore array line of the IWAVES experiment. Thin lines are the M_2 tidal characteristics emanating from locations with critical slopes ($\alpha = c$). The open circles and asterisks mark the locations of the subsurface maxima in semidiurnal-band $\langle u^2 \rangle$ and the sharp 180° phase shift in u, respectively, at the 120-, 350-, and 500-m moorings of the summer of 1997. (b) Near-bottom buoyancy period estimated from CTD casts (open circles) and fit to a third-order polynomial of water depth (line). (c) Bottom slope α and M_2 internal wave characteristic slope c near the sea bed. Characteristic slopes were estimated using the buoyancy periods near the sea bed shown in Figure 3b. In regions where a plane internal wave would be reflected forward (subcritical regions), c is plotted with a thin line, and in regions where a plane wave would be reflected backward (supercritical regions), c is plotted with a thick line. The dotted lines indicate mooring locations.

(Figure 3a), 67–80% of the water column was covered by the ADCPs. On the slope ($H > 120$ m), the full water column could not be sampled because of ADCP range limitations. In 1996, the bottom half of the water column was sampled at the 350 m mooring. In 1997, two ADCPs (a deep upward-looking, and a shallow downward-looking) were deployed on the 350 and 500 m mooring lines. Together, they covered roughly the upper 50% of the water column at each mooring. The orientation of cross-shore, u, and alongshore, v, currents were defined by the local bathymetry at each mooring. Thus, coordinates shift slightly from mooring to mooring as the isobaths incline relative to true north (Figure 1).

[11] Four to twelve temperature loggers (TLs) were distributed on the mooring lines, and bottom-mounted and near-surface pressure sensors were deployed on some of the moorings. Hourly-averaged sea level fluctuations off of San Diego (32°42.9′N 117°10.4′W) were obtained from the UH Sea Level Center/National Oceanographic Data Center Joint Archive for Sea Level. Wind speed and direction was monitored from Scripps Institution of Oceanography (SIO) pier (∼12 km north of the study site). Finally, conductivity-temperature-depth (CTD) profiles were carried out continuously at the mooring locations on numerous occasions for periods ranging from 4 to 24 hours in order to obtain information on temporal and spatial changes in stratification.

[12] The region we have defined as the shelf (H = 0 to 120 m) is ∼10 km wide at the study site (Figures 1 and 3). The bottom profile is approximately linear, deepening offshore with a slope of approximately 0.01. The continental slope topography is more complex, having a shallow bank to the southwest (which shoals to a depth of approximately 125 m), and dropping off precipitously at the Coronado Escarpment. La Jolla Canyon impinges on the shelf approximately 14 km to the north of the study site, considerably changing the shelf geometry there. Seaward of the narrow shelf to approximately 250 km offshore, the California Borderland topography contains deep basins and shallow banks before dropping to abyssal depths at the Patton Escarpment.

[13] We define the semidiurnal band to be between 1/14.5 and 1/11 cycles per hour (cph). This band is wide enough to span all the semidiurnal lines and the variance of the spectral peaks and shoulders of the observed semidiurnal variance [*Lerczak*, 2000]. We exclude the diurnal band from our analyses, because we have shown elsewhere [*Lerczak et al.*, 2001] that diurnal band motions at the IWAVES study site were dominated by diurnal wind-driven internal waves, and were not generated by the surface tide.

[14] Buoyancy frequencies were as high as 0.5 cycles per minute (cpm) at the pycnocline and as low as 0.03 cpm in the deep waters on the slope. Using all the CTD casts from the IWAVES experiments, we estimated the buoyancy frequency near the sea floor at different cross-shore locations along the mooring array. These data were fit to a third order polynomial of water depth (H) which was used to estimate the bottom buoyancy period as a function of H and distance offshore (Figure 3b). The slope of M_2 internal wave characteristics c along the bottom were then calculated according to

$$c = \frac{\sqrt{\sigma^2 - f^2}}{\sqrt{N^2 - \sigma^2}} \approx \frac{\sqrt{\sigma^2 - f^2}}{N}, \tag{3}$$

where σ is the M_2 frequency and N is the buoyancy frequency near the bottom at a particular location [*Regal and Wunsch*, 1973]. Characteristics of the M_2 frequency emanating from regions of critical bottom-slope are plotted in Figure 3a. The slope of the M_2 internal wave characteristic near the bottom and the bottom slope are plotted versus cross-shore distance in Figure 3c. At the shelf break ($x \approx 12$ km), the bottom slope was much steeper than the M_2 characteristic slope ($\alpha/c \gg 1$). This region may

serve as a natural boundary separating the slope and shelf internal wave dynamics. On either side of this region, the bottom slope was marginally subcritical ($\alpha < c$).

3. Vertical Structure of Semidiurnal Currents

3.1. Current Variance

[15] The vertical structure of semidiurnal-band current variance varied significantly from the slope to the shelf over a cross-shore range of just 16 km. On the slope, the most striking features were the large alongshore variances $\langle v^2 \rangle$ near the surface and bottom at the 350 m mooring (Figure 4d). Near the bottom (summer 1996 deployment), RMS alongshore currents were 5.5 cm s^{-1} and maximum semidiurnal currents exceeded 15 cm s^{-1}. At the surface (summer 1997), RMS alongshore currents were 4.3 cm s^{-1} and the maximum amplitude was about 12 cm s^{-1}. A secondary mid-column maximum in $\langle v^2 \rangle$ was apparent in both the summer of 1996 and 1997 at about 175 m water depth. In contrast, cross-isobath variance $\langle u^2 \rangle$ was considerably weaker (Figure 4c). Near the bottom, for example, $\langle v^2 \rangle$ was 26.5 times greater than $\langle u^2 \rangle$. Cross-isobath variance increased towards the surface, with maxima at the surface and at a depth of about 100 m, approximately the depth of the shelf break and approximately 75 m above the mid-depth maximum of $\langle v^2 \rangle$. At the depths of overlapping data from the two summer 350-m mooring deployments (150 to 190 m from the surface) the variances were comparable, suggesting the vertical structure from the two deployments was representative of typical summer conditions. At the 500 m mooring (Figures 4a and 4b), semidiurnal variances were smaller compared to the 350 m mooring. As at the 350 m mooring, $\langle v^2 \rangle$ was enhanced at the surface of the 500 m mooring, relative to mid-column, but not as dramatically.

[16] At the 120-m mooring and in the upper 120 m at the 350-m mooring (above the dashed lines in Figures 4c and 4d), the vertical structure of $\langle u^2 \rangle$ and $\langle v^2 \rangle$ were similar. We will show that the currents and temperature fluctuations from these two moorings were highly coherent.

[17] On the shelf (H = 0 to 100 m, Figures 4g–4n), the structure of the currents was notably different from the slope. Cross-shore currents were energetic and had the vertical structure expected for mode-one internal waves; minimum at mid-column and maximum near the top and bottom of the water column. In the summer of 1997, for example, the RMS u was 6.2 cm s^{-1} near the bottom at the 30-m isobath, with a maximum amplitude of 16 cm s^{-1}. In contrast, alongshore currents were largest near the surface and decayed monotonically with depth. This pattern was consistently observed for all shelf moorings and for all deployments.

[18] Seasonal changes in vertically-averaged variances, $\overline{\langle u^2 \rangle}$ and $\overline{\langle v^2 \rangle}$, were apparent on the shelf (Table 1 and Figure 4). At the 15- and 30-m moorings, $\overline{\langle u^2 \rangle}$ was slightly greater in the summer than in the fall. In contrast, $\overline{\langle v^2 \rangle}$ was slightly greater in the fall than in the summer. As a consequence, $\overline{\langle v^2 \rangle} < \overline{\langle u^2 \rangle}$ during the summer (on average, $\overline{\langle v^2 \rangle}/\overline{\langle u^2 \rangle} = 0.60$, standard deviation (s.d.) = 0.10, n = 6) while $\overline{\langle v^2 \rangle} \approx \overline{\langle u^2 \rangle}$ during the fall (on average, $\overline{\langle v^2 \rangle}/\overline{\langle u^2 \rangle} = 1.08$, s.d. = 0.18, n = 4). However, for both seasons, the variance ratio was greater than what would be expected for an internal tide propagating in the cross-shore direction ($f^2/\sigma^2 = 0.31$, see equation (2)).

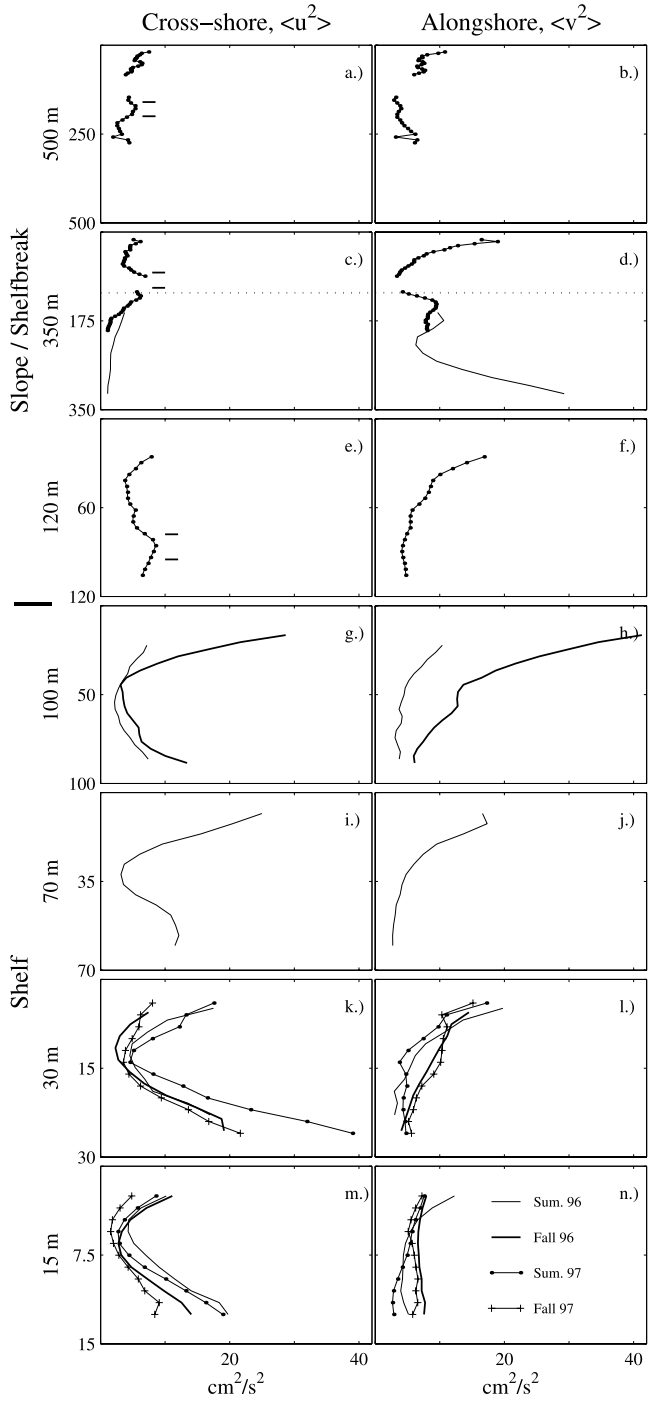

Figure 4. Semidiurnal-band horizontal current variance versus depth from ADCPs deployed at different water depths during the 1996 and 1997 IWAVES field studies. Variance curves from different deployments are indicated by different line types. The horizontal dashed lines in Figures 4c and 4d mark a depth of 120 m. The short pairs of horizontal lines in Figures 4a, 4c, and 4e mark the range of the subsurface maximum in $\langle u^2 \rangle$ referred to in the text and in Figure 3.

[19] Seasonal changes at the 100-m mooring were more dramatic. Both $\overline{\langle u^2 \rangle}$ and $\overline{\langle v^2 \rangle}$ were 2 to 4 times greater in the fall than the summer of 1996.

Table 1. Depth-Averaged, Semidiurnal Kinetic Energy[a]

Mooring Depth, m	$\overline{\langle v^2 \rangle}$ cm^2 s^{-2},	$\overline{\langle u^2 \rangle}$ cm^2 s^{-2}
Summer 1996, 25 June to 29 August, Slope		
350	11.4	1.71
Summer 1996, 25 June to 29 August, Shelf		
100	4.21	3.77
70	6.98	10.4
30 s	6.10	9.23
30 c	6.36	8.85
30 n	6.02	10.1
15	5.36	9.80
Fall 1996, 26 September to 1 November, Shelf		
100	15.6	8.79
30	9.13	9.49
15	7.57	6.96
Summer 1997, 28 June to 17 August, Slope		
500 u	7.58	5.02
500 l	3.96	3.76
350 u	6.98	3.75
350 l	5.36	2.58
Summer 1997, 28 June to 17 August, Shelf		
120	5.93	4.71
30	5.74	13.0
15	4.54	7.18
Fall 1997, 3 September to 17 October, Shelf		
30	8.24	8.80
15	5.85	4.36

[a]Vertically-averaged, semidiurnal-band, alongshore and cross-shore variance ($\overline{\langle v^2 \rangle}$ and $\overline{\langle u^2 \rangle}$, respectively) during the 1996 and 1997 IWAVES field studies. Variances for each deployment were estimated over common time ranges (except for the 15-m mooring in the summer of 1996, for which the range was 27 July to 29 August). The letters c, n, and s designate moorings deployed at, north of, and south of the central onshore/offshore mooring line. In 1996, n and s moorings at the 30-m isobath were approximately 1.2 and 0.66 km, respectively, from the central mooring. ADCPs were at the bottom, looking upward, except that the letters u and l indicate where upper (downward looking) and lower (upward looking) ADCPs, respectively, were deployed in the summer of 1997.

[20] The vertical structure of semidiurnal currents at all moorings was not like that expected for the surface tide, that is, uniform variance with depth. RMS amplitudes were considerably larger than the surface tidal currents ($\sim$1 to 2 cm s^{-1}) off the southern California coast reported by *Munk et al.* [1970] and, as noted above, showed strong vertical variability. *Winant and Bratkovich* [1981] noted that vertically-averaged tidal band currents observed on the shelf off Del Mar (Figure 1) were intermittent and were not modulated by the spring/neap cycle of the surface tide. We conclude that semidiurnal variability at the IWAVES study site was dominated by the internal tide.

3.2. Relative Phase of $\vec{u}$

[21] The squared coherency, ρ^2, and vertical change in phase, $\Delta\phi$, of u and v versus depth were calculated using the cross-spectra, $S_{u(zo)u(z)}$ and $S_{v(zo)v(z)}$, between the currents measured at a mooring at a particular reference depth, z_o, and the currents at all other depths z (Figures 5 and 6). The cross-spectra were averaged over the semidiurnal band and over the four ADCP bins surrounding the reference depth. Relative phases are positive when the currents at z lead the currents at z_o. For each mooring, we calculated the relative phase for several reference depths. The value of $\Delta\phi$ was dependent on z_o. However, the vertical variations in $\Delta\phi$ were roughly independent of the reference depth. For example, at the 120-m mooring, $\Delta\phi_{v/v}$ had similar vertical variations for z_o = 32 and 100 m (Figure 5d). The roughly 40° offset between the two curves was due to the phase difference between v at the two reference depths (v at z = 32 m led v at z = 100 m by about 40°).

[22] For all slope and shelfbreak moorings, $\Delta\phi_{u/u}$, had a single sharp 180° phase shift in the water column. Consider, for example, $\Delta\phi_{u/u}$ at the 350 m mooring from the summer of 1997 with z_o equal to 80 m (Figure 5f, pluses). Moving up in the water column from mid-depth, $\Delta\phi_{u/u}$ changed linearly from 180° to 0° (upward phase propagation). It remained constant at 0° until it abruptly shifted to −180° at z = 50 m. The sharp 180° phase shift in u also occurred at $z \approx 50$ at the 120-m mooring (Figure 5b). However, at the 500 m mooring, the 180° phase shift occurred much deeper in the water column ($z \approx 205$ m; Figure 5j).

[23] In contrast to the cross-shore currents, the phase in the alongshore currents, $\Delta\phi_{v/v}$, varied smoothly and changed very little with depth. At the three slope and shelfbreak moorings, $\Delta\phi_{v/v}$ did not change by more than about 90° in the vertical, and there were no sharp phase shifts (Figures 5d, 5h, and 5l).

[24] Below mid-column at the 350-m mooring (from the summer of 1996), both $\Delta\phi_{u/u}$ and $\Delta\phi_{v/v}$ vary smoothly with depth. For similar reference depths from the 1996 and 1997 summer deployments ($z_o \approx 180$ m, circles and squares in Figures 5e–5h), $\Delta\phi_{u/u}$ and $\Delta\phi_{v/v}$ had similar slopes and connected smoothly over the region of overlap, again suggesting that the semidiurnal internal wave environment at this location was similar during the two summers.

[25] On the shelf (Figure 6) the vertical structure of $\Delta\phi_{u/u}$ and $\Delta\phi_{v/v}$ was consistent from mooring to mooring and for each deployment. Here, z_o was from the average depth of the bottom four ADCP bins for u and the upper four ADCP bins for v. For u, $\rho^2_{u/u}$ was maximum near the bottom (as expected since z_o was near the bottom). It dipped to near zero at mid-column (where $\langle u^2 \rangle$ was minimum) and rose back to nearly the maximum value towards the surface. Relative phase was nearly constant at the bottom, and shifted sharply by 180° at the same depth as the minimum in $\rho^2_{u/u}$. The depth of this phase shift was at mid-column or slightly higher. This is consonant with a mode-one internal wave. The $\Delta\phi_{u/u}$ at the 100 m mooring in the fall of 1996 (Figure 6n, thick line) contrasted somewhat from this description. Here, there was a 180° phase change from top to bottom. However, the variation was smooth with depth and did not have a sharp 180° phase shift at mid-depth.

[26] For alongshore currents, $\rho^2_{v/v}$ was maximum near the surface (as expected since z_o was near the surface and $\langle v^2 \rangle$ was large near the surface) and decreased to near-zero values near the bottom. Unlike $\Delta\phi_{u/u}$, and inconsistent with a mode-one internal wave model, $\Delta\phi_{v/v}$ was nearly constant with depth at all moorings and all deployments, and did not have a sharp 180° phase shift.

4. Coherence and Relative Phase Between the Slope and Shelfbreak

[27] To test whether the internal tide propagated across the slope and shelfbreak, we calculated the relative phase

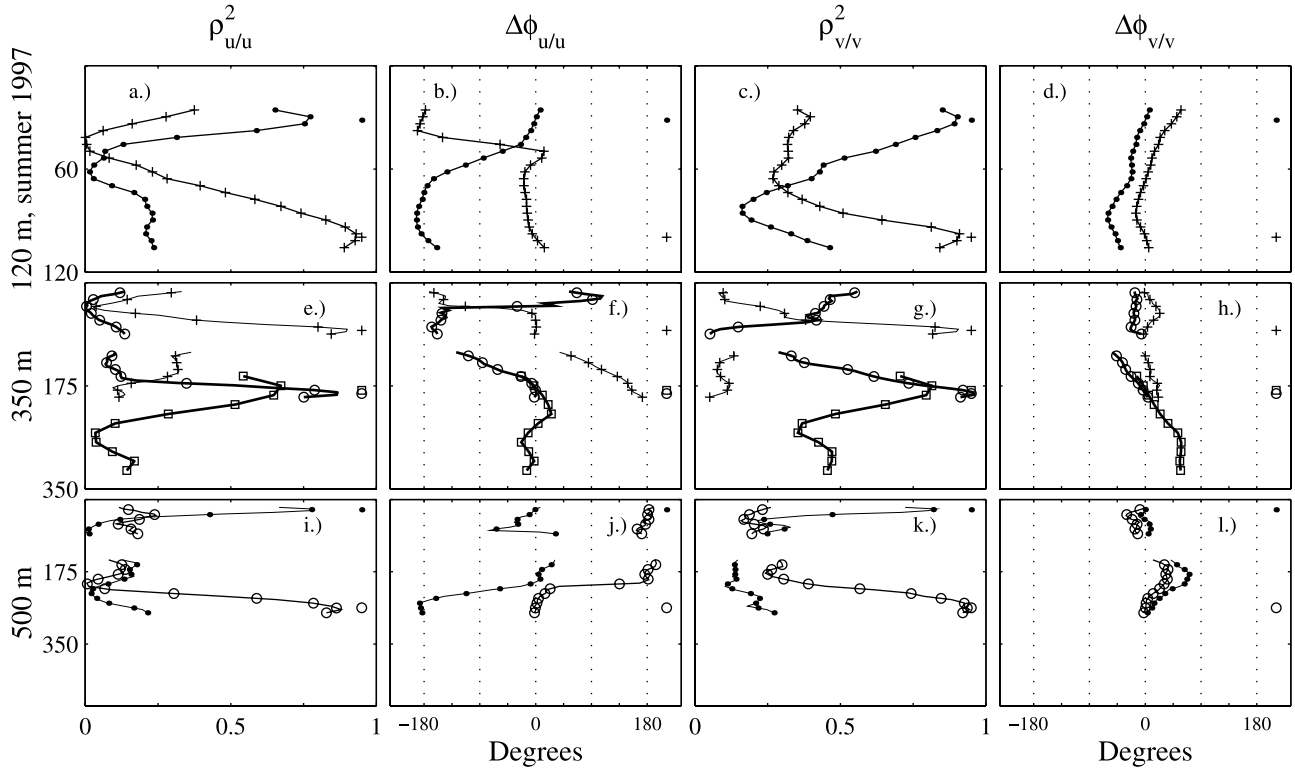

Figure 5. Semidiurnal-band coherency-squared, $\rho^2_{u(z0)/u(z)}$ and $\rho^2_{v(zo)/v(z)}$, and vertical change in phase, $\Delta\phi_{u(zo)/u(z)}$ and $\Delta\phi_{v(zo)/v(z)}$, between currents at a fixed reference depth z_o indicated by the symbols at the right side of each panel, and currents at all ADCP bin depths z. (a–d) The120-m mooring from the summer of 1997. (e–h) The 350-m mooring from the summer of 1996 (squares) and summer of 1997 (all other symbols). (i–l) The 500-m mooring from the summer of 1997. The thick lines in Figures 5e–5h were used to highlight ρ^2 and $\Delta\phi$ when similar reference depths were used for the 1996 and 1997 data at the 350-m mooring. Relative phase is positive when the currents at z lead the currents at z_o.

and squared coherency between currents at the 350- and 120-m moorings from the summer of 1997, separated by a cross-shore distance of 2.0 km (Figure 7). Squared coherencies were very high between currents at roughly the same depth at the two moorings. At these depth pairs, $\rho^2_{u/u}$ and $\rho^2_{v/v}$ both had maximum values of 0.84 (Figure 7b). The relative phases between currents at equal depths at the two moorings (Figure 7a) drifted slightly with depth, but remained very close to zero (average $\Delta\phi_{u/u}$ was $-8.5°$ (std. dev. 9.3°) and average $\Delta\phi_{v/v}$ was 5.8° (std. dev. 5.2°)). On average, neither $\Delta\phi_{u/u}$ nor $\Delta\phi_{v/v}$ were significantly different from zero, and we conclude that the semidiurnal currents were coherent, but did not propagate across the slope and shelfbreak. An exception is the cross-shore currents at z = 70 to 85 m for which the average $\Delta\phi$ was $-21°$, corresponding to an offshore cross-shore phase speed of 77 cm s^{-1}, comparable to the phase speed of a long flat-bottom, mode-one internal wave, which we estimated for the conditions observed at the shelfbreak.

[28] Squared coherency of semidiurnal-band temperature variability between temperature loggers at different slope and shelfbreak moorings was also high. For the four uppermost temperature loggers at the 350- and 120-m moorings in the summer of 1997 (z = 10, 22, 34, and 46 m), $\rho^2_{T/T}$ was 0.61, 0.87, 0.80, and 0.87, respectively, calculated between temperature loggers at equal depths at the two moorings. However, unlike u and v, which were in phase at equivalent depths (Figure 7a), T at the 350-m mooring tended to lead T at the 120-m mooring by roughly 60° ($\Delta\phi_{T/T}$ = 53°, 64°, 52°, and 66°, respectively).

5. Coherence and Relative Phase Across the Shelf

[29] We now address the question of whether the semidiurnal internal tide propagated in the cross-shore direction on the shelf. For u, we calculated the relative phase and squared coherency between the near-bottom ADCP bins of adjacent cross-shelf moorings on the shelf and shelfbreak. For v, the near-surface ADCP bins were used ($\langle v^2 \rangle$ was greatest at the surface, Figure 4). Relative phase, $\Delta\phi$, was converted to a temporal lag Δt according to $\Delta t = T_{M2}\,\Delta\phi/360°$, where T_{M2} is the M_2 period. Temporal lags were divided by the cross-shore distance Δx between the moorings, giving an estimate of the inverse cross-shore phase speed c_p^{-1} of the semidiurnal signal, which is positive for onshore phase propagation. Results are summarized in Figure 8.

[30] Semidiurnal-band squared coherency between near-bottom u of neighboring moorings on the shelf were high (Figure 8b), and phase lags were always positive (onshore phase propagation). At mid-shelf ($\gg$3 km from the coast), c_p^{-1} ranged from 0.7–1.3 s m^{-1}, corresponding to a phase speed c_p range of 80–140 cm s^{-1} (somewhat faster than the

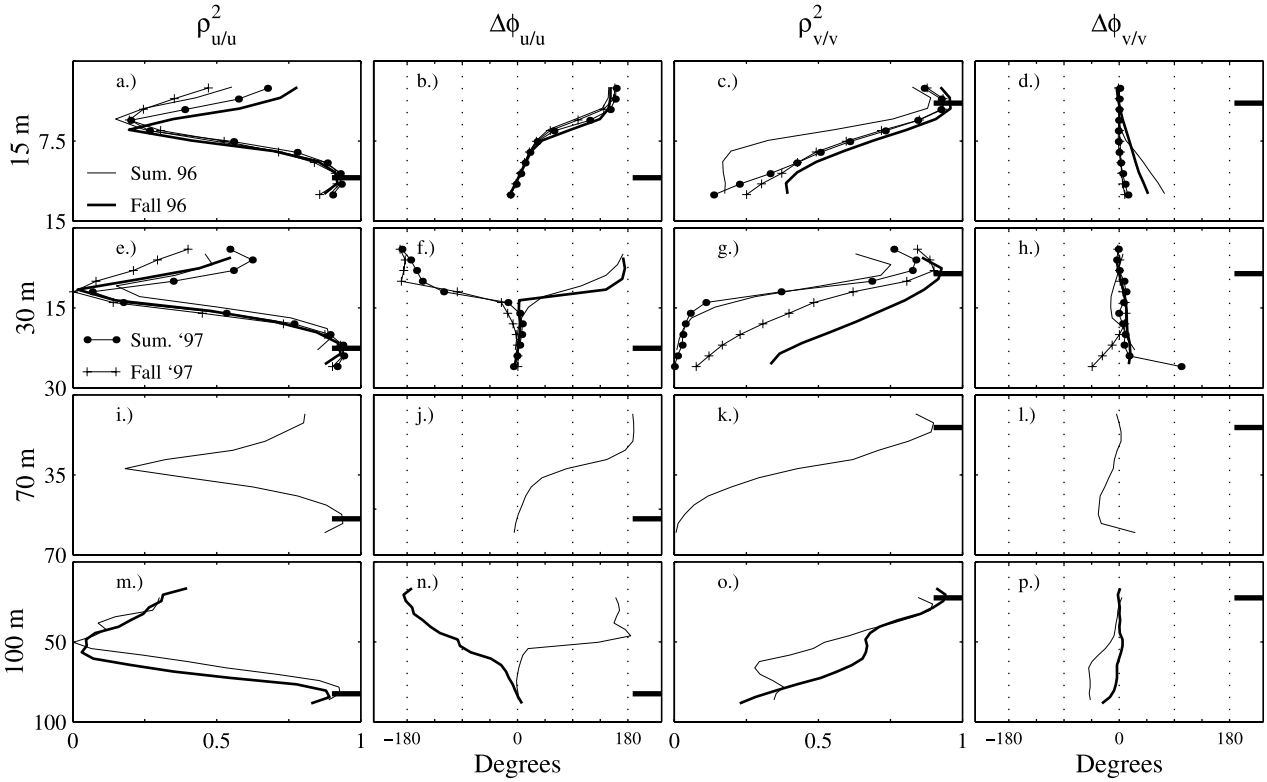

Figure 6. Semidiurnal-band coherencies-squared, $\rho^2_{u/u}$ and $\rho^2_{v/v}$, and relative phases, $\Delta\phi_{u/u}$ and $\Delta\phi_{v/v}$, between currents at a fixed depth, z_o (marked by a bold horizontal line on the right side of each panel) and currents at all ADCP bin depths z from the shelf moorings of the IWAVES field studies: (a–d) 15-m mooring, (e–h) 30-m mooring, (i–l) 70-m mooring, and (m–p) 100-m mooring. Different symbols correspond to different deployments.

phase speed of a freely-propagating, mode-one, M_2 internal wave at mid-shelf which we estimate to be 50 cm s^{-1}).

[31] Nearer to the coast (<3 km), c_p^{-1} was more variable and had a clear seasonal dependence. For the summer deployments, c_p^{-1} ranged from 0.6–2.4 s m^{-1}. While for the fall deployments, c_p^{-1} ranged from 3.5–5.2 s m^{-1}. In the summer, the corresponding c_p range (40–170 cm s^{-1}) was faster than that for a freely-propagating mode-one internal wave (≈18 to 32 cm s^{-1} for H = 15 to 30 m). While in the fall, c_p (20–30 cm s^{-1}) was comparable to that of a freely-propagating mode-one internal wave.

[32] The squared coherency of near-surface v between adjacent moorings (Figure 8d) was not as high as that of near-bottom u. At mid-shelf, c_p^{-1} was scattered about zero (Figure 8c). Closer to shore, c_p^{-1} was apparently positive, however, there was not a clear seasonal pattern.

[33] The relative phase between mid-column T (used as a proxy for mid-column isopycnal displacement) and current can be used to determine the direction of internal wave propagation and distinguish between progressive and standing internal waves. For a mode-one internal wave propagating towards the coast, mid-column T and bottom u are 180° out of phase and mid-column T lags surface v by 90°. For a mode-one internal wave that is standing in the cross-shore direction, mid-column T leads bottom u by 90° and mid-column T and upper v are 180° out of phase (within a quarter wavelength of the coast).

[34] Semidiurnal-band relative phase and squared coherency between u near the bottom of the water column and T from the mid-column temperature loggers at shelf moorings are summarized in Figure 9. At each shelf mooring, we use temperature loggers deployed at roughly H/3 and 2H/3 [*Lerczak*, 2000] for this calculation.

[35] For all moorings, $\Delta\phi_{u/T}$ was between 97° and 144°. At the 30- and 15-m moorings, $\rho^2_{u/T}$ was particularly high ($\gg$0.7). The squared coherency between v (near the surface) and T was somewhat lower than that for u and T, particularly at the 15-m mooring. At the 70- and 30-m moorings, $\Delta\phi_{v/T}$ was scattered about 180°. At the 15-m mooring, however, $\Delta\phi_{v/T}$ was about 135° during the fall of 1996 (the single deployment for which $\rho^2_{v/T} \gg 0.2$).

[36] While the vertical structure of u on the shelf was consistent with a mode-one internal wave (Figures 4 and 6), the phase relationship between u and mid-column T was neither consistent with a purely onshore progressive (bottom u 180° out of phase with T) nor a purely standing (bottom u ± 90° out of phase with T) flat-bottom, mode-one internal wave. For H = 15–70 m, $\Delta\phi_{u/T}$ was 20–30° higher than 90° and was somewhat higher in the fall than in the summer. For example, the average nearshore ($H \leq$ 30 m) $\Delta\phi_{u/T}$ was 107° (s.d. 7°, n = 8) for the summer deployments and 121° (s.d. 13°, n = 8) for the fall deployments.

6. Semidiurnal Time Series

[37] We now present semidiurnal band-passed time series at selected moorings and depths (Figure 10) in order to

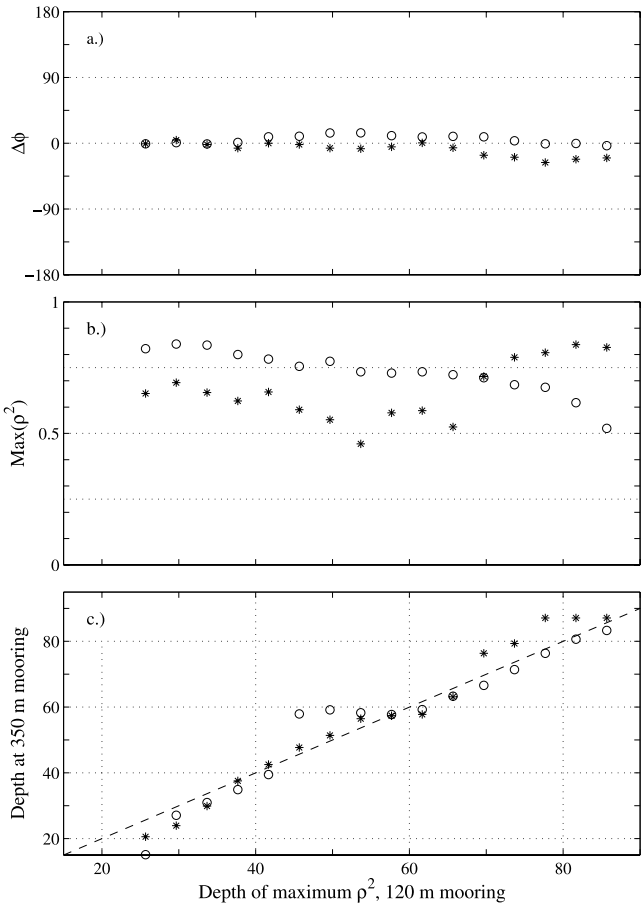

Figure 7. (a) Squared coherency, ρ^2, and (b) relative phase, $\Delta\phi$, between currents at the 350- and 120-m moorings during the IWAVES experiment of the summer of 1997. Asterisks (circles) are for ρ^2 and $\Delta\phi$ between u (v) at the two moorings. Values shown in Figures 7a and 7b are for each depth bin of the ADCP at the 120-m mooring and at the corresponding depth bin at the 350-m mooring for which ρ^2 was maximum. (c) The depth bin used at the 350-m mooring for each 120-m mooring depth bin.

assess the degree of intermittency of the semidiurnal currents. While we only show time series from the summer deployment of 1996, the conclusions discussed here were drawn from observations from all deployments. We first determine, qualitatively, the degree to which the time series tracked the spring/neap modulation of the surface tide. Second, we assess the correspondence of time series from moorings separated by different cross-shore and alongshore distances. Finally, we assess whether the changes in internal tide energy were associated with local changes in stratification.

[38] Typically, time series on the shelf did not track the spring/neap cycle of the surface tide. Like the time series observed by *Winant and Bratkovich* [1981] and *Bratkovich* [1985], the IWAVES currents behaved qualitatively like narrow-band processes. They were modulated at roughly a 2-week or faster timescale, but did not beat regularly as did the surface tide, which contains only discrete harmonics. In the summer of 1996, for example, the cross-shore currents on the shelf were comparatively weak until about day 210 (Figure 10a). Afterward, a series of four energetic pulses passed over the shelf.

[39] The alongshore currents near the bottom of the 350 m mooring of the summer of 1996 (Figure 10b) were an exception. There the modulation of v closely matched that of the surface tide, and the spring/neap cycle was apparent.

[40] Time series in close proximity to each other corresponded well. For example, the currents from the central and northern moorings along the 30-m isobath (1.2 km separation) were nearly identical. Correspondence between currents became weaker as the cross-shore separation

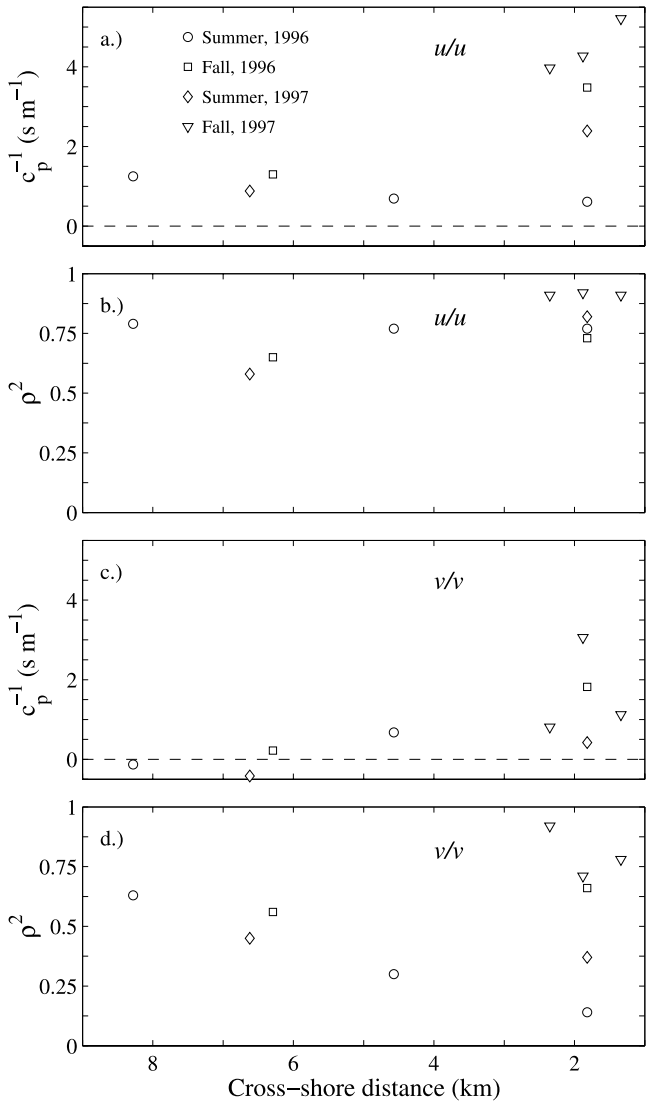

Figure 8. Semidiurnal-band temporal phase lag per unit cross-shore distance (inverse cross-shore phase speed c_p^{-1}) estimated for (a) u at the deepest ADCP bin and (c) v at the bin nearest to the surface between adjacent cross-shelf moorings during the IWAVES field studies. (b, d) Corresponding squared coherencies for u and v, respectively. The x-axis shows the average cross-shore distance of the moorings used to estimate the phase lag. Phase lags are positive when the offshore mooring leads the onshore (onshore phase propagation). When $\rho^2 < 0.2$, the corresponding c_p^{-1} is not plotted.

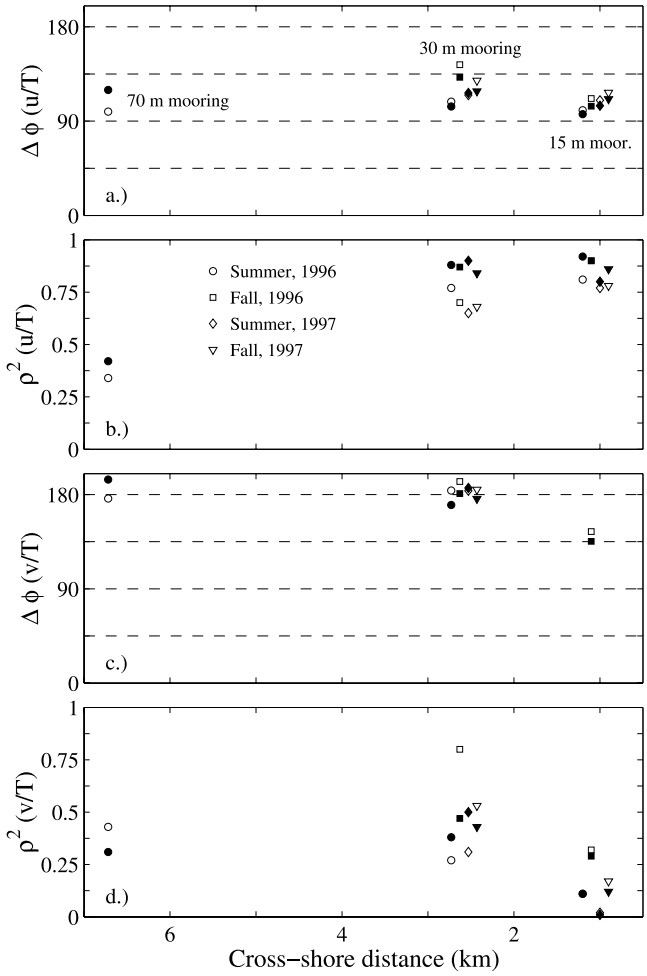

Figure 9. Semidiurnal-band relative phase between mid-column temperature fluctuations and (a) u at the near-bottom ADCP bin and (c) v at the near-surface ADCP bin for shelf moorings of the IWAVES field studies. (b, d) Corresponding squared coherencies for u and v, respectively. The x-axis indicates the cross-shore location of the mooring. Different deployments (different symbols) have been shifted slightly from the true cross-shore location to avoid overlap of points. Open (solid) symbols are for the temperature loggers at $z = H/3$ ($z = 2H/3$). Phase lags are positive when T leads the current. When $\rho^2 < 0.2$, the corresponding c_p^{-1} is not plotted.

increased. However, currents across the shelf had similar patterns of modulation.

[41] Seasonal and higher frequency changes in stratification were apparent in the upper 250 m of the water column during IWAVES. However, the shelf and slope waters were well-stratified throughout the experiments, with a strong pycnocline at a depth of 5 to 10 m with a buoyancy frequency ranging from 0.25 to 0.5 cycles per minute. To assess the variability in stratification over the summer of 1996, we plot the vertical change in temperature, ΔT, over that upper 100 m of the water column at the 350 and 100 m moorings in the summer of 1996 (Figure 10). This vertical change in temperature was well-correlated between the two moorings (over the time period when the two time series overlapped), and ranged from 8° to 12°. Variations in ΔT over the summer of 1996, however, were not correlated with the large variations in internal tide current amplitude.

7. Discussion

7.1. Coastal Trapped Waves on Slope and Shelfbreak

[42] We propose that, on the slope and shelfbreak, the semidiurnal variability is dominated by northward-propagating, topographically-trapped internal waves. At subinertial frequencies, the currents of coastal-trapped waves at the continental margin tend be oriented in the alongshore direction [*Huthnance*, 1978; *Ou*, 1980; *Ou and Beardsley*, 1980; *Dale et al.*, 2001]. When the internal deformation radius is large compared to the cross-shore lengthscale of the continental slope, the coastal-trapped waves tend to behave like Kelvin waves: cross-shore currents nearly zero, alongshore currents having a modal internal wave structure (for example, for a mode-one Kelvin wave, v near the surface is 180° out of phase with v near the bottom), propagating in a direction with the coast to the right (in the Northern Hemisphere), and decaying offshore at roughly the internal deformation radius. For conditions observed at $H = 500$ m at the IWAVES study site, we estimate the long, mode-one, internal wave phase speed to be 100 cm s^{-1}, giving a deformation radius (c_p/f) of 13 km, larger than the width of the slope (~5 km).

[43] As the frequency of a coastal-trapped wave increases, the alongshore wavelength goes to zero and the wave becomes bottom trapped at the slope [*Rhines*, 1970]. The maximum allowed frequency for these waves is $N\alpha$, where α is the maximum slope of the cross-shore bottom profile. Using the bottom buoyancy period and bottom slope of Figures 3b and 3c, we estimate the maximum $N\alpha$ to be 0.43 cycles per hour (period = 2.3 hours) at 11.7 km from the coast ($H = 240$ m).

[44] *Huthnance* [1978], *Dale and Sherwin* [1996] and *Dale et al.* [2001] have shown that, at superinertial frequencies, perfectly-trapped coastal modes cannot exist. Energy is scattered into freely-propagating internal waves. However, at frequencies close to the inertial frequency, energy will be "nearly" trapped to the coast [*Chapman*, 1982a, 1982b; *Dale and Sherwin*, 1996; *Dale et al.*, 2001]. These waves have the form of their subinertial counterparts, but lose energy to free internal waves as they propagate away from their source.

[45] On the slope ($H = 350$ m), $\langle v^2 \rangle$ was much greater than $\langle u^2 \rangle$ and current ellipses at the top and bottom of the water column were aligned in the alongshore direction. Some aspects of the structure of the currents at this mooring were like a mode-one internal Kelvin wave (flow predominantly aligned in the alongshore direction, maximum at the top and bottom of the water column, and minimum at mid-depth (Figures 4k and 4l)). However, the $\Delta\phi_{v/v}$ between different vertical separations at the 350-m mooring from the summers of 1996 (bottom half of water column) and 1997 (upper half) (Figure 5h) varied smoothly, without a sharp 180° phase shift, as would be expected for a mode-one Kelvin wave. *Ou and Beardsley* [1980] have shown that alongshore currents of subinertial bottom-trapped waves (BTW) near a continental margin can have a nearly vertically-uniform, slowly-varying phase over the slope.

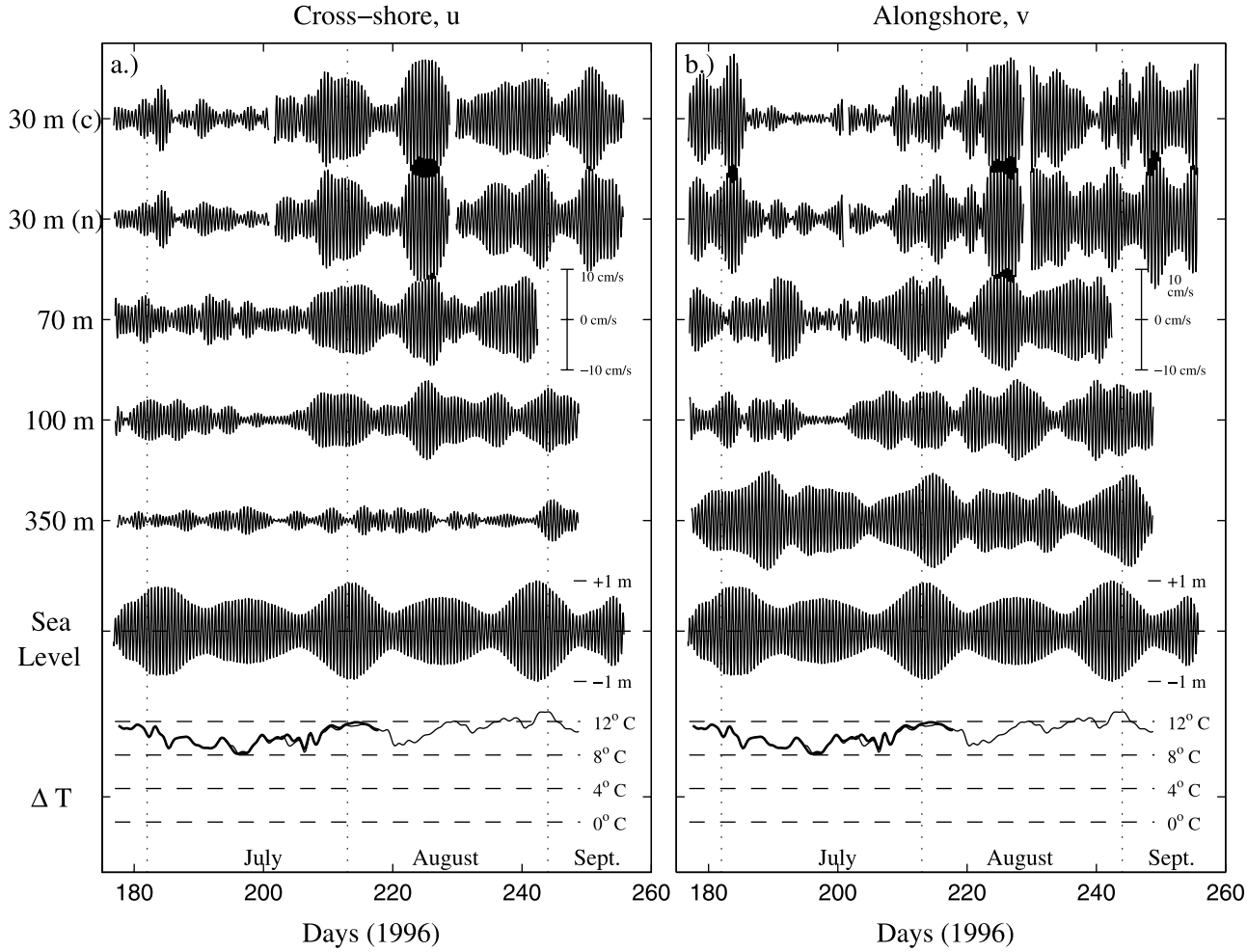

Figure 10. Time series of semidiurnal band-passed ($\frac{1}{14.5}$ to $\frac{1}{11}$ cph) (a) cross-shore and (b) alongshore currents at selected moorings from the summer of 1996 IWAVES deployment. For H = 30, 70 and 100 m, u is plotted for ADCP bins near the bottom of the water column (z = 23, 60 and 86 m, respectively) and v is plotted for near-surface ADCP bins (z = 5, 8, and 22 m, respectively). For H = 350 m, both u and v are plotted for z = 287 m. Time series are plotted for both the central (c) and northern (n) ADCPs located on the 30-m isobath (alongshore separation = 1.2 km). Semidiurnal band-passed sea level variability is plotted at the bottom of each panel, as well as low-passed (frequencies < 1/33 cph) vertical temperature difference, ΔT, at selected moorings. ΔT was calculated between z = 1 and 94 m at the 350-m mooring (thick line); and between z = 1 and 88 m at the 100-m mooring (thin line).

[46] *Huthnance and Baines* [1982] also observed enhanced alongshore semidiurnal variance at the top and bottom of the water column on the steep continental slope (H = 500 m) off the northwest coast of Africa. They attempted, with limited success, to model the bottom-intensified currents as a combination of up-slope and down-slope propagating BTWs [*Rhines*, 1970]. If the up- and down-slope waves have equal amplitudes, the motions will be standing in the cross-slope direction and progressive in the alongslope direction, with shallower water to the right when facing the direction of propagation. The wave will have the following form:

$$\begin{aligned} u' &= iA\cos(\theta)\cos(k'x')e^{ily-\kappa z'+imz'-i\sigma t}, \\ v &= A\sin(\theta)\sin(k'x')e^{ily-\kappa z'+imz'-i\sigma t}, \end{aligned} \tag{4}$$

where A is the amplitude of the wave and x' points in the upslope direction and z' is normal to the sloping seafloor. The current u' is oriented along the x' axis. The angle θ is determined by

$$\theta = \cos^{-1}\left(\frac{\sigma}{N\alpha}\right). \tag{5}$$

Near the bottom of the 350-m mooring, the buoyancy period was ~30 min and the bottom slope α was ~0.07. For the M_2 frequency, θ is 55°.

[47] The alongshore and up-slope currents are 90° out of phase with respect to each other, and the polarization can be either clockwise or counterclockwise depending on the cross-slope location. The minor to major ellipse axis ratio is given by

$$\epsilon^{-1} = \frac{|u|}{|v|} = \frac{1}{\tan(\theta)\tan(k'x')}, \tag{6}$$

where ε^{-1} is positive when the polarization is clockwise and negative when the polarization is counterclockwise.

[48] According to *Rhines* [1970],

$$l = \kappa \cos(\theta) \frac{\cos(\beta)^2 + S^2 \sin(\beta)^2 \sin(\theta)^2}{S\left(1 - \sin(\beta)^2 \cos(\theta)^2\right)},$$
$$k' = \kappa \sin(\theta) \frac{\cos(\beta)^2 + S^2 \sin(\beta)^2 \sin(\theta)^2}{S\left(1 - \sin(\beta)^2 \cos(\theta)^2\right)}, \quad (7)$$

where $S = N/f \approx 44.4$ and $\beta = \arctan(\alpha)$. Below a depth of 200 m at the 350-m mooring, $|v|$ decays towards the surface with a vertical decay length scale, κ^{-1}, of approximately 120 m (Figure 11). This gives alongshore and cross-slope wavelengths of 8 and 5 km, respectively.

[49] The currents near the bottom at the 350-m mooring were consistent with this BTW model. The estimated cross-slope wavelength ($\lambda_x \approx 5$ km) is comparable to the width of the slope region suggesting that the motions may be associated with a wave trapped on the slope. The alongshore wavelength ($\lambda_y \approx 8$ km) is short, and there are topographic features to the south of the IWAVES study site of comparable scale that might be the source of the motions (for example, the bank just to the south, Figure 1).

[50] In this BTW model, when the currents are counterclockwise circularly polarized, as was observed near the bottom at the 350-m mooring, v and T will be 180° out of phase. This was what we observed near the bottom of the 350-m mooring, where v led T by 176° ($\rho^2_{v/T} = 0.72$) at a depth of 311 m. Below 125 m, the isopycnal displacements were very large, with peak to trough displacements exceeding 60 m. In the BTW model, currents are parallel to the slope at all depths and large advective displacements would be expected, as was observed in the numerical studies of *Ou and Beardsley* [1980].

[51] The currents at the same depths at the 120- and 350-m moorings of the summer of 1997 were remarkably coherent (Figure 7). The relative phase of currents at equal depths between the two moorings was small and could not be distinguished from zero cross-shore phase propagation (particularly for $z < 75$ m). This supports our proposal that energy on the slope is predominantly standing in the cross-shore direction and propagating in the alongshore direction. Squared coherency of T at equal depths between the 120- and 350-m moorings was also high. However, the 60° relative phase between temperature loggers at equal depths suggests that a nodal line in T was crossed between the 120- and 350-m moorings.

7.2. Shelf Variability

[52] On the shelf, both alongshore and cross-shore variances were large. Cross-shore variance had the vertical structure of a mode-one internal wave (maxima at the top and bottom of the water column with surface currents 180° out of phase with bottom currents). In contrast, alongshore currents were surface-enhanced and decayed monotonically toward the bottom. The phase of v was roughly constant with depth.

[53] At the shelfbreak ($H = 100$ m), the variance of the semidiurnal currents increased by over a factor of four from the summer to the fall of 1996. Closer to shore, the seasonal changes in variance were apparent, but were not as appreciable as at the 100-m mooring.

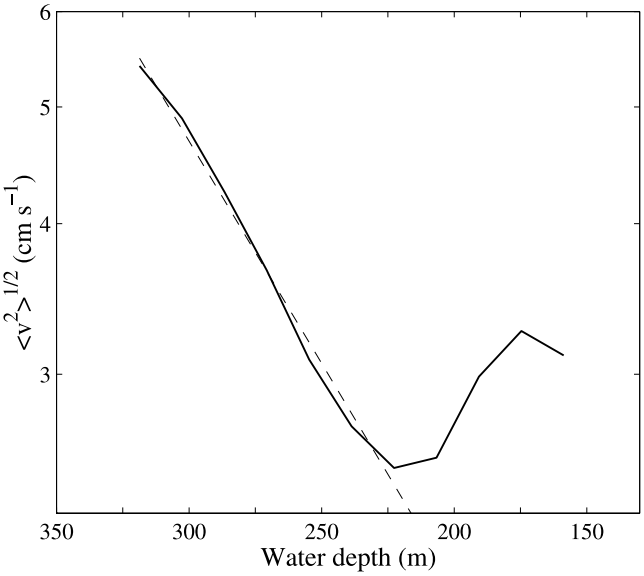

Figure 11. RMS amplitude of the alongshore currents v (log scale) from the 350-m mooring of the summer of 1996 versus depth. The linear (dashed) curve is a least-squares fit of the data below 220 m. The slope of the line is an estimate of the vertical decay scale κ of v ($\kappa^{-1} \approx 120$ m).

[54] On the shelf, the near-bottom u propagated towards the coast for all deployments. At $H < 30$ m, the phase speed was higher in the summer than in the fall. The relative phase between near-bottom u and mid-column T on the shelf ranged from 97°–144°, and was consistent with neither a purely-standing ($\Delta\phi_{u/T} = 90°$) nor a purely-progressive ($\Delta\phi_{u/T} = 180°$) mode-one internal wave. At $H < 30$ m, $\Delta\phi_{u/T}$ tended to be greater in the fall than in the summer deployments. We conclude that the semidiurnal u on the shelf is a partially-reflected wave. Seasonal changes in cross-shore phase speed and $\Delta\phi_{u/T}$ were both consistent with the reflection coefficient being larger in the summer than in the fall.

7.3. Semidiurnal Current Intermittency

[55] Near the bottom of the 350-m mooring in the summer of 1996, the alongshore currents tracked the spring/neap cycle of the surface tide and their power spectrum closely resembled that of the surface tide (see *Lerczak* [2000] for details). Sharp M_2 peaks with N_2 and S_2 peaks rising above the background were also observed for S_v at the 100-m mooring in the fall of 1996 and the 350-m mooring (near-surface v) in the summer of 1997. For most of the moorings, however, semidiurnal band currents were intermittent and were not modulated by the spring/neap cycle. Long periods (~25 days) of low semidiurnal energy were followed by pulses of high internal tide energy which was modulated on fortnightly and shorter timescales. Despite the intermittency of the semidiurnal-band currents, their vertical structure on the shelf was remarkably stable.

[56] The semidiurnal variability at the IWAVES study site was dominated by the internal tide. However, the phase of the alongshore currents did not vary in the vertical, despite very large vertical changes in the amplitude of alongshore currents. This implied that the internal tidal currents had a

nonzero mean, making it impossible to separate the internal tidal variability from the weaker surface tidal currents. The method of separating the surface tidal currents from the baroclinic by taking a vertical mean must, therefore, be used with caution, particularly in regions with significant topographic variation like the narrow continental shelf and slope in southern California.

[57] The semidiurnal-band currents on the slope and shelf observed during IWAVES were intermittent at most (but not all) locations and behaved like a narrow-band process. However, the structure of the variability was stable from one deployment to the next, but was not easily interpreted as purely mode-one internal waves or coastal-trapped waves. A detailed numerical study (for example, like those of *Cummins and Oey* [1997] and *Merrifield et al.* [2001]) would complement our study, and seems necessary to understand how the evanescent and propagating internal tide interrelate in the vicinity of realistic (and complicated) bathymetry.

[58] **Acknowledgments.** The IWAVES field program and subsequent analysis effort has been funded by the Office of Naval Research. The authors wish to thank Lou Goodman for his support. We also thank Charles Coughran, Paul Harvey and Jerry Wanetick for their help in mooring development and deployment, instrument maintenance, data collection and maintenance, and computer support. Thanks are also owed to Dave Chapman for his careful review of the manuscript.

References

Baines, P. G., Internal tides, internal waves and near-inertial motions, in *Baroclinic Processes on Continental Shelves*, *Coastal Estuarine Sci.*, vol. 3, edited by C. N. K. Mooers, pp. 19–31, AGU, Washington, D. C., 1986.

Bratkovich, A., Aspects of the tidal variability on the southern California shelf, *J. Phys. Oceanogr.*, *15*, 225–239, 1985.

Cairns, J. L., Asymmetry of internal tidal waves in shallow coastal waters, *J. Geophys. Res.*, *72*, 3563–3565, 1967.

Chapman, D. C., Nearly trapped internal edge waves in a geophysical ocean, *Deep Sea Res.*, *29*, 525–533, 1982a.

Chapman, D. C., On the failure of Laplace's tidal equations to model subinertial motions at a discontinuity in depth, *Dyn. Atmos. Ocean.*, *7*, 1–16, 1982b.

Colosi, J. A., R. C. Beardsley, J. F. Lynch, G. Gawarkiewicz, C.-S. Chiu, and A. Scotti, Observations of nonlinear internal waves on the outer New England continental shelf during the summer Shelfbreak Primer study, *J. Geophys. Res.*, *106*, 9587–9601, 2001.

Cummins, P. F., and L. Y. Oey, Simulation of barotropic and baroclinic tides off northern British Columbia, *J. Phys. Oceanogr.*, *27*, 762–781, 1997.

Dale, A. C., and T. J. Sherwin, The extension of baroclinic coastal-trapped wave theory to superinertial frequencies, *J. Phys. Oceanogr.*, *26*, 2305–2315, 1996.

Dale, A. C., J. M. Huthnance, and T. J. Sherwin, Coastal-trapped internal waves and tides at near-intertial frequencies, *J. Phys. Oceanogr.*, *31*, 2958–2970, 2001.

Denbo, D. W., and J. S. Allen, Rotary empirical orthogonal function analysis of currents near the Oregon coast, *J. Phys. Oceanogr.*, *14*, 35–46, 1984.

Hayes, S. P., and D. Halpern, Observations of internal waves and coastal upwelling off the Oregon coast, *J. Mar. Res.*, *34*, 247–267, 1976.

Holloway, P. E., Observations of internal tide propagation on the Australian north west shelf, *J. Phys. Oceanogr.*, *24*, 1706–1716, 1994.

Holloway, P. E., P. G. Chatwin, and P. Craig, Internal tide observations from the Australian north west shelf in summer 1995, *J. Phys. Oceanogr.*, *31*, 1182–1199, 2001.

Huthnance, J. M., On coastal trapped waves: Analysis and numerical calculation by inverse iteration, *J. Phys. Oceanogr.*, *8*, 74–92, 1978.

Huthnance, J. M., and P. G. Baines, Tidal currents in the northwest African upwelling region, *Deep Sea Res.*, *29*, 285–306, 1982.

La Fond, E. C., Internal waves, I, in *The Sea*, vol. 1, *Physical Oceanography*, pp. 731–751, Wiley-Intersci., New York, 1962.

Lerczak, J. A., Internal waves on the southern California shelf, Ph.D. thesis, Univ. of Calif., San Diego, La Jolla, Calif., 2000.

Lerczak, J. A., M. C. Hendershott, and C. D. Winant, Observations and modeling of coastal internal waves driven by a diurnal seabreeze, *J. Geophys. Res.*, *106*, 19,715–19,729, 2001.

Merrifield, M. A., P. E. Holloway, and T. M. S. Johnston, Internal tide generation at the Hawaiian Ridge, *Geophys. Res. Lett.*, *28*, 559–562, 2001.

Munk, W., F. Snodgrass, and M. Wimbush, Tides off-shore: Transition from California coastal to deep-sea waters, *Geophys. Fluid Dyn.*, *1*, 161–235, 1970.

Ou, H. W., On the propagation of free topographic Rossby waves near continental margins, 1, Analytical model for a wedge, *J. Phys. Oceanogr.*, *10*, 1051–1060, 1980.

Ou, H. W., and R. C. Beardsley, On the propagation of free topographic Rossby waves near continental margins, 2, Numerical model, *J. Phys. Oceanogr.*, *10*, 1323–1339, 1980.

Regal, R., and C. Wunsch, M_2 tidal currents in the western North Atlantic, *Deep Sea Res.*, *20*, 493–502, 1973.

Rhines, P., Edge-, bottom-, and Rossby waves in a rotating stratified fluid, *Geophys. Fluid Dyn.*, *1*, 273–302, 1970.

Rosenfeld, L. K., Baroclinic semidiurnal tidal currents over the continental shelf off northern California, *J. Geophys. Res.*, *95*, 22,153–22,172, 1990.

Sherwin, T. J., Analysis of an internal tide observed on the Malin Shelf, north of Ireland, *J. Phys. Oceanogr.*, *18*, 1035–1050, 1988.

Torgrimson, G. M., and B. M. Hickey, Barotropic and baroclinic tides over the continental slope and shelf off Oregon, *J. Phys. Oceanogr.*, *9*, 945–961, 1979.

Winant, C. D., and A. W. Bratkovich, Temperature and currents on the southern California shelf: A description of the variability, *J. Phys. Oceanogr.*, *11*, 71–86, 1981.

Winant, C. D., and J. R. Olson, The vertical structure of coastal currents, *Deep Sea Res.*, *23*, 925–936, 1976.

Wunsch, C., Internal tides in the ocean, *Rev. Geophys.*, *13*, 167–182, 1975.

M. C. Hendershott and C. D. Winant, Center for Coastal Studies, 0209, Scripps Institution of Oceanography, La Jolla, CA 92093-0209, USA. (mch@coast.ucsd.edu; cdw@coast.ucsd.edu)

J. A. Lerczak, Department of Physical Oceanography, MS 21, Woods Hole Oceanographic Institution, Woods Hole, MA 02543, USA. (jlerczak@whoi.edu)